https://doi.org/10.1186/s40517-022-00241-3

Geothermal Energy

RESEARCH

Open Access

Investigating high permeable zones in non-volcanic geothermal systems using lineament analysis and fault fracture density (FFD): northern Konawe Regency, Indonesia

Daffa Arrofi, Israa S. Abu-Mahfouz* and Sinatrya Diko Prayudi

*Correspondence: israa.abumahfouz@kfupm.edu.sa

Department of Geosciences, College of Petroleum Engineering and Geosciences, King Fahd University Petroleum and Minerals, Dhahran, Saudi Arabia

Abstract

Indonesia has high geothermal potential comprising 40% of the world's potential geothermal energy, volcanic and non-volcanic systems. Volcanic systems have witnessed more exploration activities for geothermal resources compared to non-volcanic systems. A high potential non-volcanic system in Indonesia is located in the northern part of Konawe, Southeast Sulawesi. Previous research had identified surface temperature anomaly (high temperature) and some surface manifestations for this area, specifically in the northeast part of Wawolesea. However, the source of surface manifestations and permeable zones as an implication of a good reservoir are still unknown. Therefore, this research aims to investigate the permeable zones and geothermal potential in the non-volcanic geothermal system of north Wawolesea by applying lineaments analysis and the fault fracture density (FFD) method. A total of 1694 major and minor lineaments were manually delineated using ArcGIS based on Digital Elevation Model Nasional (DEMNAS). FFD map and rose diagrams displayed the orientation of all lineaments and structures with the major lineaments trending NNE–SSW, whereas the minor lineaments showed irregular distribution and orientation. Field measurements also show the same azimuth orientation for the mapped fractures. Five zones were characterized by high FFD values (2.81–4.54 km/km^2). One of the extensively fractured zones (Zone C) is located between Meluhu and Lembo, covering an area of around 19.39 km^2. This area is interpreted to be highly permeable and suggestive of a recharge area that contributes to surface manifestation in the Wawolesea. Therefore, the area between Meluhu and Lembo in the northern part of Konawe shows high geothermal potential due to its planar morphology and high FFD values. This study allows an improved understanding of how fracture geometry, distribution and density control the permeability in geothermal reservoirs.

Keywords: Northern part of Konawe, Lineament analysis, Fault fracture density (FFD), Digital Elevation Model Nasional (DEMNAS), Geothermal energy, Permeability

Introduction

The conventional energy supply is decreasing by the day, and the energy demand nowadays has necessitated seeking more alternative energy. One of the alternative energies is geothermal energy; in its broad term, the thermal energy contained in our planet (Manzella 2017). This energy comes from the Earth's natural heat, primarily due to the decay of uranium, thorium, and potassium (Dickson and Fanelli 2004). According to Naivasha (2015), geothermal resources can be found worldwide, but an exploitable geothermal system is mainly found in regions of high geothermal gradients. Generally, these exploitable areas are associated with Earth's plate boundaries and volcanic regions. Nevertheless, they are sometimes also found as warm groundwater in sedimentary formations worldwide and the heat flux to the surface. Based on their nature and geological setting, geothermal systems can be categorized into two major types: volcanic geothermal systems and non-volcanic geothermal systems (Naivasha 2015).

Indonesia is located at the confluence of three major tectonic plates: Eurasia, Indo-Australia, and the Pacific, which provides a huge contribution to the availability of geothermal energy in the country. Geothermal resources in Indonesia are estimated at 40% of the world's potential geothermal resources (Suharmanto et al. 2015). However, most of the exploration was conducted on volcanic geothermal systems and only a few studies have been done on non-volcanic systems (e.g., Suryantini and Wibowo 2010; Suryantini 2013; Nahli et al. 2016), although the country is considered promising for non-volcanic geothermal systems. A potential non-volcanic geothermal system is located in the northern part of Konawe, Southeast Sulawesi (Idral 2010). The results obtained from processing remote sensing data revealed high surface temperature and surface manifestations in the northeast part of Wawolesea (Jaya et al. 2021). Such a manifestation may indicate fluid transmission in the geothermal system through faults and fractures. Generally, faults and fractures created by tectonic processes in geothermal systems can serve as a pathway for geothermal fluids (Siler et al. 2019). Besides, faults and fractures play an important role in fluid circulation in the geothermal reservoirs (Chen et al. 2021). This study attempts to identify the faults and fractures in the potential non-volcanic geothermal system in the northern part of Konawe through a comprehensive lineament and fault fracture density (FFD) analysis using remote sensing data. The location of the study area and the identified surface manifestations in the northern part of Konawe are provided in Fig. 1.

Lineament analysis is key to interpreting regional-to-subregional scale structures from remote sensing (Dasgupta and Mukherjee 2019). Any natural linear features on the Earth's surface related to extension/compression/strike-slip or resulted from of igneous or metamorphic activities are termed lineaments (Prost 2013). Lineaments are simple or composite linear surface features whose parts are aligned in a rectilinear or slightly curvilinear relationship and differ distinctly from the pattern of adjacent feature and presumably reflects a subsurface phenomenon (Allum 1978). By analyzing the orientation trend of azimuth lineaments, the fluid source supplying surface manifestation can be predicted. In addition, identifying high permeable zones will help identify good recharge and geothermal reservoir areas. This study aims to address the following research questions:

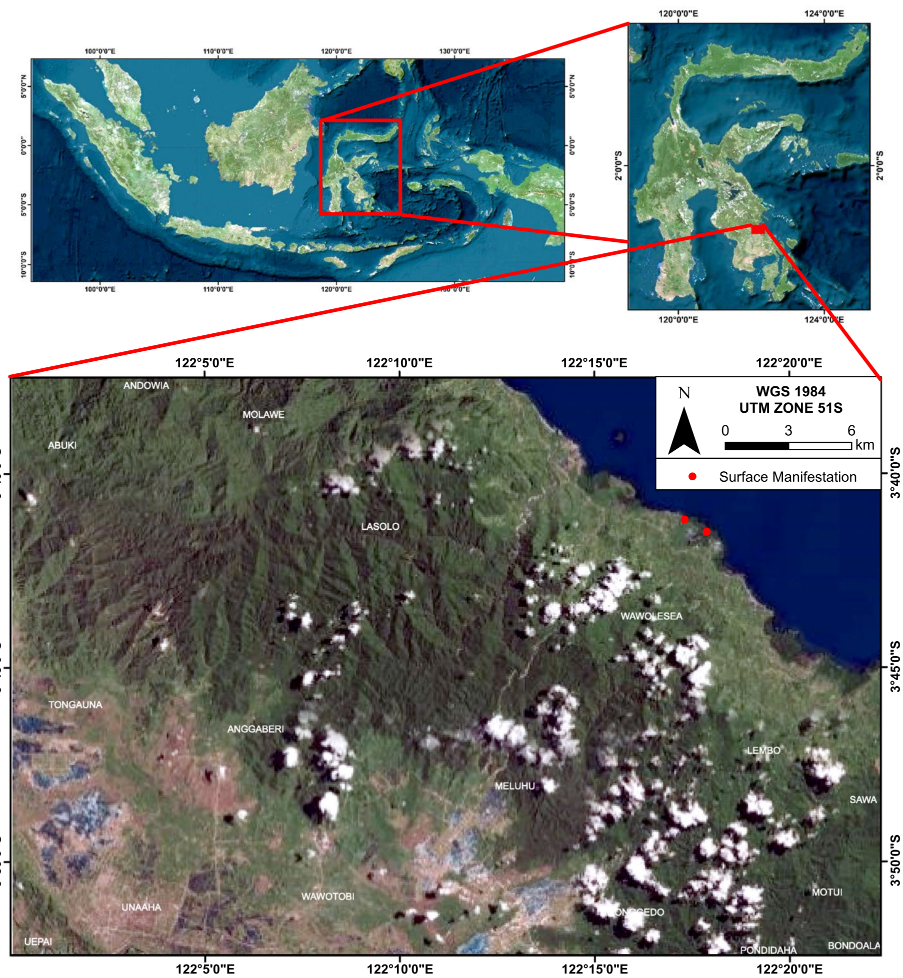

Fig. 1 Microsoft Bing map showing the location of study area in the northern part of Konawe (Data source: Microsoft Bing 2022)

1. What is the main azimuth orientation of the lineaments in the northern part of Konawe and what is the source direction of surface manifestation in the northeast part of Wawolesea?
2. Which areas are considered high permeable zones in the northern part of Konawe and their implications as a good reservoir area?
3. Where is the location of the prospective geothermal reservoir based on lineament analysis and FFD (fault fracture density) values?

Geological framework

According to Nahli et al. (2016), Sulawesi is situated at the intersection of three major plates: the Eurasian, Indo-Australian, and Pacific. Consequently, the tectonic activities resulted in the development of both volcanic and non-volcanic geothermal systems in Sulawesi, (Nahli et al. 2016). Based on Idral (2010) study, the volcanic geothermal systems are mainly located in the north arm of Sulawesi, while the non-volcanic geothermal systems are dominantly located in other arms (central part of Sulawesi, south arm, and southeast arm of Sulawesi). In the southeastern arm of Sulawesi, the non-volcanic geothermal systems are distributed in 14 areas (Idral 2010). Among them one is located in the northern part of Konawe. Those potential geothermal systems are probably controlled by active tectonic events. In the Southeast arm of Sulawesi, the main structure formed after the collision was the shear faulting, including the Matarombeo fault, the Lawanopo fault system, the Konawe fault system, the Kolaka fault, as well as many other faults and lines (Hamimu et al. 2019). Among these faults, the Lawanopo fault is the main fault system that lies within the study area (Fig. 2).

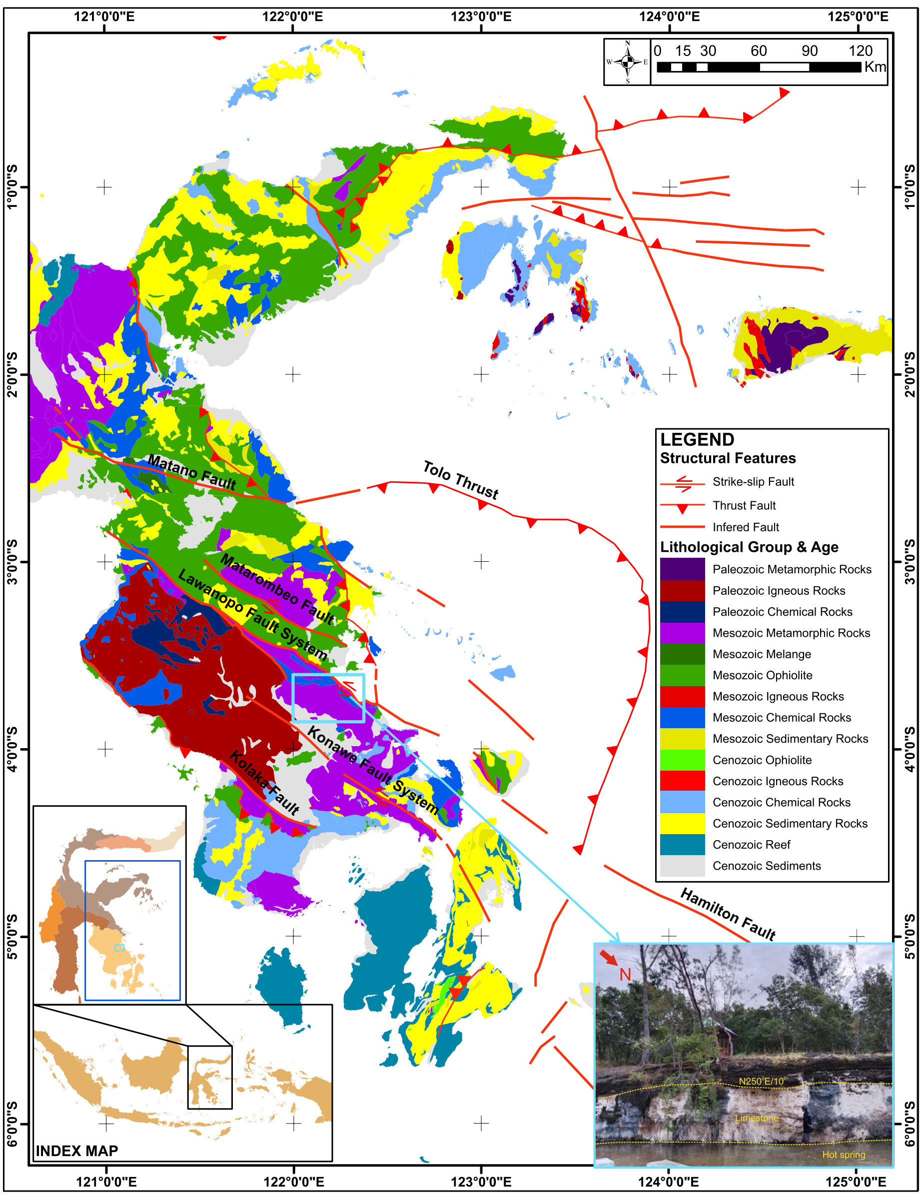

Fig. 2 Map showing the Lawapono fault system in the southeast Sulawesi (Simandjuntak et al. 1993; Martosuwito 2012; Surono and Simandjuntak 1993; Tjokrosapoetra et al. 1993). Blue rectangle outlines the study area

Based on a geological map by Rusmana et al. (1993), there are four rock units in the area (from the oldest to the youngest): Paleozoic metamorphic rocks (Schist, Gneiss, Phyllite, Quartzite, Slate, and Marble), Tokala Formation (calcilutite, limestone, sandstone, shale, marl, and slate), Meluhu Formation (sandstone, quartzite, black shale, red shale, phyllite, slate, limestone, and siltstone), and alluvial sediments (pebble, gravel, sand, and clay) (Fig. 3). Among those units, the Meluhu Formation is the intensely affected by faults with a NE–SW orientation.

According to previous research by Jaya et al. (2021), anomalous surface temperature (high temperature) and geothermal manifestations exist in the northern part of Konawe. Based on LST (land surface temperature) maps, the geothermal potency is located along the coastal line of Lasolo, particularly in the Wawolesea and Toreo Village. The type of geothermal manifestation within these areas is in the form of hot springs. The temperature shown by the LST map ranges between 26.35 and 37.42 °C (Fig. 4), while the in situ temperature (geothermal manifestations) ranges from 30.2 to 65.5 °C (Jaya et al. 2021). Geochemical analyses of the hot water in the spring show that the water is of chloride water type that comes from a reservoir at a significant depth (Jamaluddin and Umar 2017; Aulia et al. 2022).

Methods

This study integrates two types of data (primary data and secondary data) to map and analyze lineaments and fault/fracture density in the non-volcanic geothermal filed of northern Konawe. Primary data were gained from DEMNAS (Digital Elevation Model Nasional) data processing, while secondary data were gained from the literature. The flowchart method of this research is provided in Fig. 5. This study utilized three software programs to process the data: ArcMap 10.8.1, Microsoft Excel 2016, and Rockwork 16.

ArcMap 10.8.1 was used to process DEMNAS; compiling six DEMNAS data into one raster, projecting DEMNAS raster data to WGS 1984 UTM Zone 51S, creating hill shade to interpret the lineament, creating lineament shapefile, calculating the density of

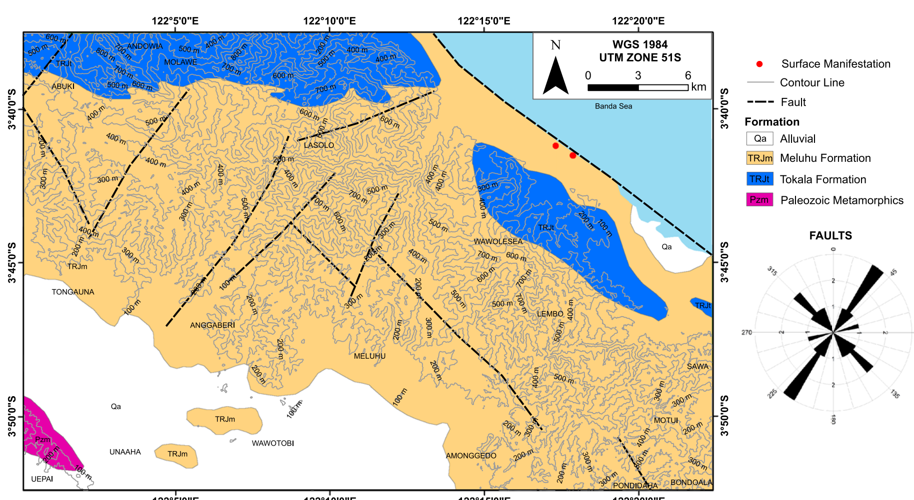

Fig. 3 Geological map of the study area. Rose diagram shows the orientation of faults in the area (Rusmana et al. 1993)

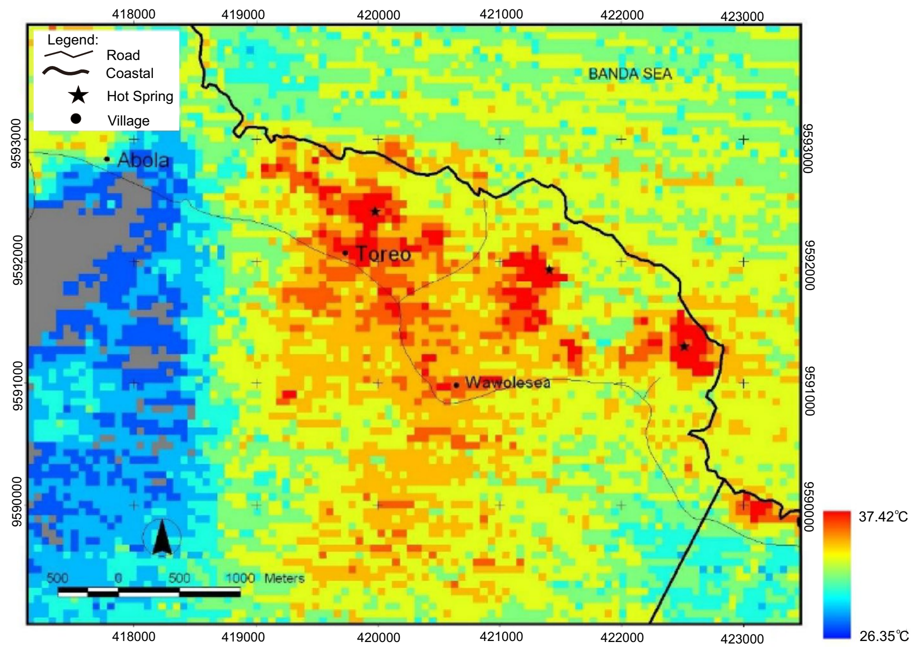

Fig. 4 LST map showing the anomaly of high surface temperature and geothermal manifestations in Toreo and Wawolesea (from Jaya et al. 2021)

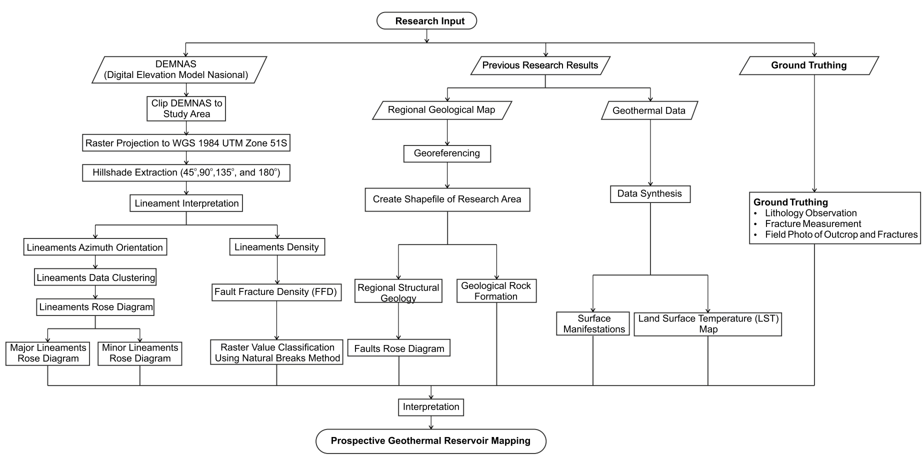

Fig. 5 Research flowchart

lineaments, and performing layout of the maps. In addition, ArcMap was also used as the tool to update the regional geological map and delineate main structural features. Microsoft Excel 2016 was used to cluster the data and generate a boxplot. Rockworks 16 was used to display the distribution of lineaments using the rose diagram of all lineaments, the major lineaments, minor lineaments and faults rose diagrams.

Six DEMNAS grid datasets were combined into one single raster data to trace lineaments and measure FFD in the study area. DEMNAS was used due to its high (0.27 arc-second) resolution compared to DEM SRTM images that have 1 arc-second resolution (BIG 2018; USGS 2018), providing more detailed images for a better processing and lineament detection. Besides DEMNAS, lineament features can be traced using multispectral image data including Landsat and Sentinel 2 satellite imagery in addition to topographic information (Abdelkareem and Al-Arifi 2021). However, most of the study areas were covered by vegetation, so tracing lineaments on the surface using a multispectral image is hard. After DEMNAS data had been combined into a single raster data, it was projected using project raster in data management tools. It was projected to WGS 1984 UTM (Universal Transverse Mercator) Zone 51S system.

The lineament extraction was performed manually to avoid extraction of non-structural line elements, such as roads and buildings (Sarp 2005). In many terrains with considerable relief, a shadowing effect (due to the particular incidence angle direction of the sunray path), may mask/obscure a few structural and geomorphic features (Fisher et al. 2012). Therefore, hill shade was created from mosaiced DEM using the 3D Analyst tool in ArcMap. Hill shade created a shaded relief from a surface raster by considering the illumination source angle and shadow. Four different angles of sun azimuth were extracted in this process; 45°, 90°, 135°, and 180°, with 30° sun latitude for each hill shade (Fig. 6), so the bias regarding sunray azimuth was reduced during interpretation.

According to Laubach et al. (2018), the most meaningful measure of fluid flow or fracture strength is the spatial arrangement of fractures at or above the threshold. Therefore, after lineaments had been interpreted, the length of lineaments should be considered as a parameter of fluid transmission.

Major and minor lineaments were plotted on different rose diagrams to identify the azimuth orientation trend of the lineaments. The density of lineaments in the research area was depicted by FFD maps. This density map was created using the density tool in ArcMap. This tool calculated the density by dividing the length by the cell area; usually,

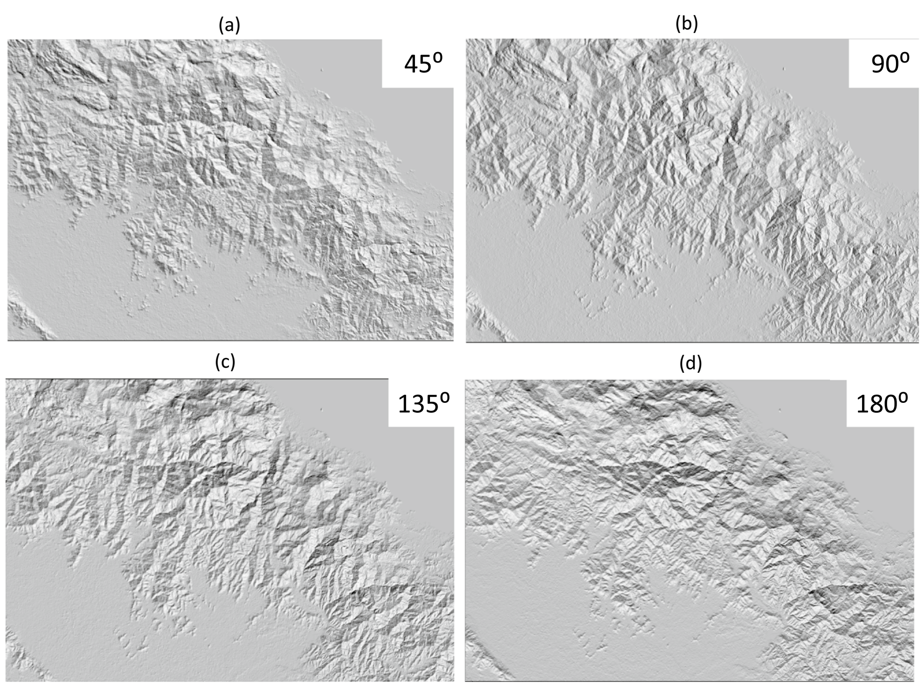

Fig. 6 Hill shade of study area from different angles of sun azimuth: **a** 45° sun azimuth, b 90° sun azimuth, **c** 135° sun azimuth, **d** 180° sun azimuth

Table 1 Summary of fracture measurements of all fractures observed in the different study localities

Location	Fracture density (m^{-1})	Type	Relative fracture orientation	Number of fractures	Average fracture aperture (mm)
GT-1	–	–	–	–	–
GT-2	NM	CV	NNE–SSW	32	2.59
GT-3	–	–	–	–	–
		OF	N–S	29	3.71
GT-4	16.21	SV	NW–SE	18	20.36
			NNE–SSW	53	11.88
GT-5	7.8	SV	NNW–SSE	25	8.6
GT-6	4.63	SF	NNW–SSE	22	–
GT-7	NM	OF	N–S	18	18.56
		SV	NNE–SSW	41	28.22
GT-8	7.5	SF	NNW–SSE and NNE–SSW	50	–

GT ground-truthing location, *CV* carbonate vein, *OF* open fracture, *SV* silica vein

the unit used is km/km^2. Then FFD results were categorized into five groups based on the range using the natural breaks method because its information loss is comparatively smaller when compared to other methods (Osaragi 2002).

To support the primary data result, geological and geothermal data were derived from the literature (e.g., Rusmana et al. 1993; Jaya et al. 2021). A regional geological map by Rusmana et al. (1993) was used as the secondary data for geological features, rock emplacement, and regional structures in the study area. Pre-defined faults in the regional geology map were plotted into a rose diagram to know the azimuth orientation and compare with the findings of the present study. In addition, surface manifestation and high-temperature anomaly of land surface temperature by Jaya et al. (2021) were synthesized to support the interpretation of potential geothermal areas.

Ground truthing fieldwork was carried out to validate the results of remote sensing and collect direct field information, including collecting field observations, mapping fractures, photography, and sampling from eight localities within the study area (Table 1). Field observations included identifying lithology and stratigraphy, measuring the main geological and structural features in the study area, and investigation the mineralogy of cemented fractures.

Results

Lineament interpretation

Based on the lineament interpretation of four sun azimuth directions, a total of 1694 lineaments were extracted in the study area (Fig. 7). The extracted lineaments were subdivided into two groups: major and minor lineaments. Boxplot diagram (Fig. 8) shows that the upper bound of minor lineaments is 1.61 km, meaning that the length of major lineament cluster is more than 1.61 km in length, while for minor lineaments it is less than 1.61 km (Fig. 8). Therefore, 67 and 1627 lineaments were measured as major and minor, respectively.

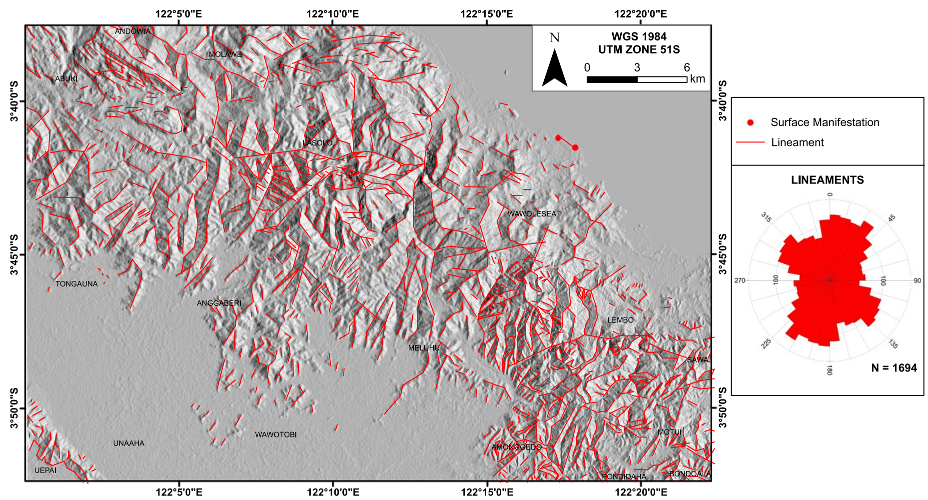

Fig. 7 Map showing the lineaments traced and interpreted in the study area

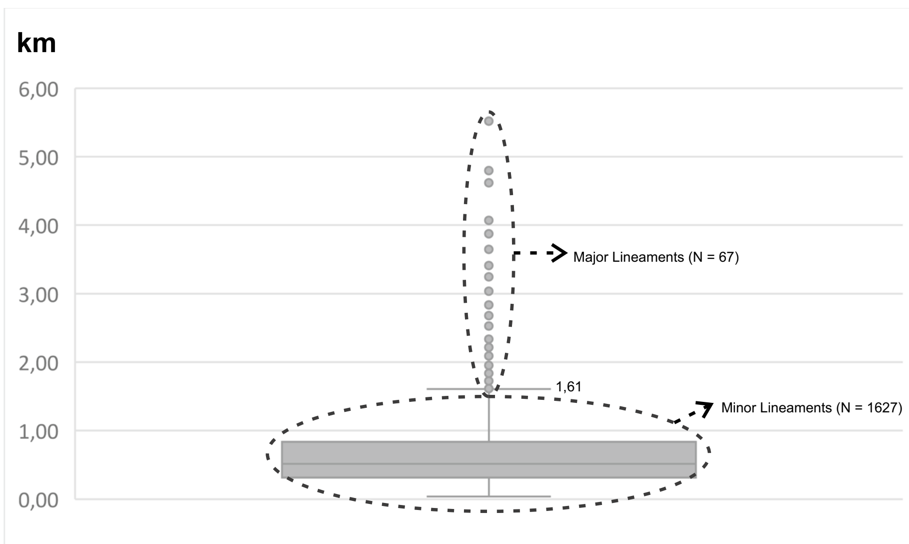

Fig. 8 Clusterization of lineament length in boxplot

Lineament azimuth orientation

Major and minor lineaments data plotted in different rose diagrams show different lineament azimuth orientations (Fig. 9). Based on 67 datasets, the rose diagram of major lineaments shows an aligned azimuth orientation of NNE–SSW trend. Four lineaments show NW–SE orientation, and the other four data show E–W orientation. In contrast, 1627 data of minor lineaments show irregular azimuth orientation in the rose diagram.

Fault fracture density (FFD)

Fault fracture density (FFD) map was generated to identify the permeable zones in the geothermal reservoir of Northern Konawe. The FFD map shows five value categories

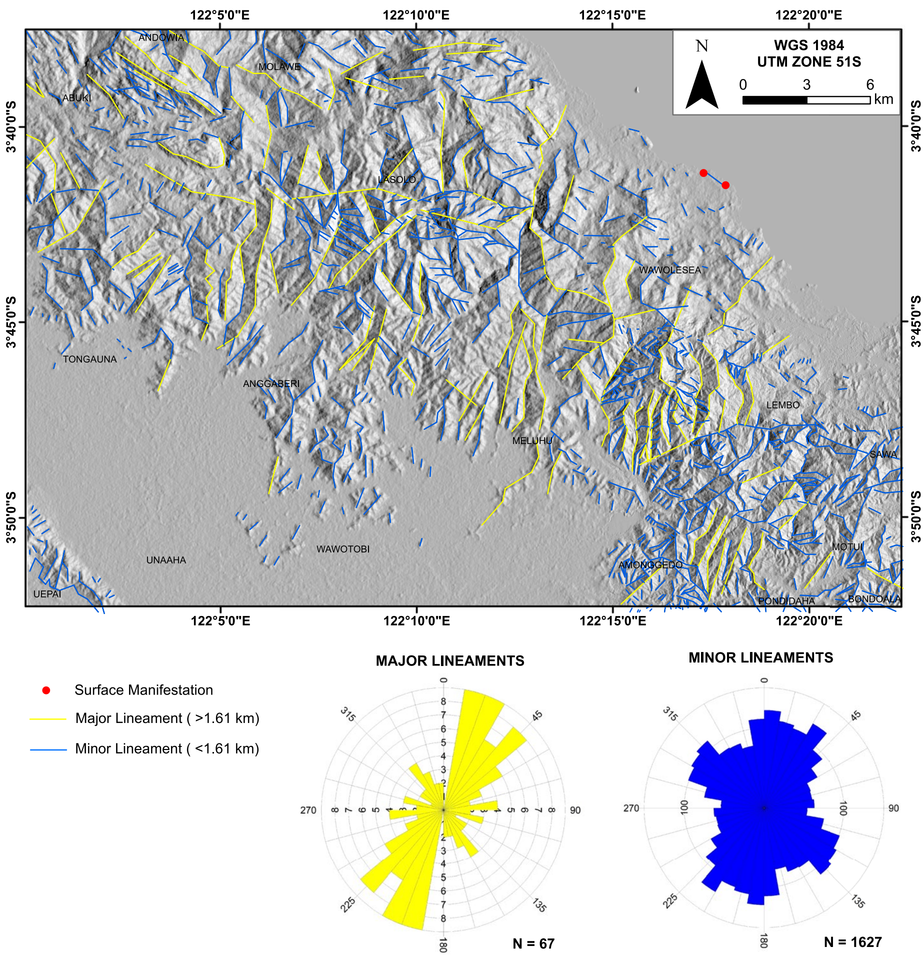

Fig. 9 Map of lineaments clusterization based on the lineaments lengths and lineament orientation (major lineament in yellow; minor lineament in blue)

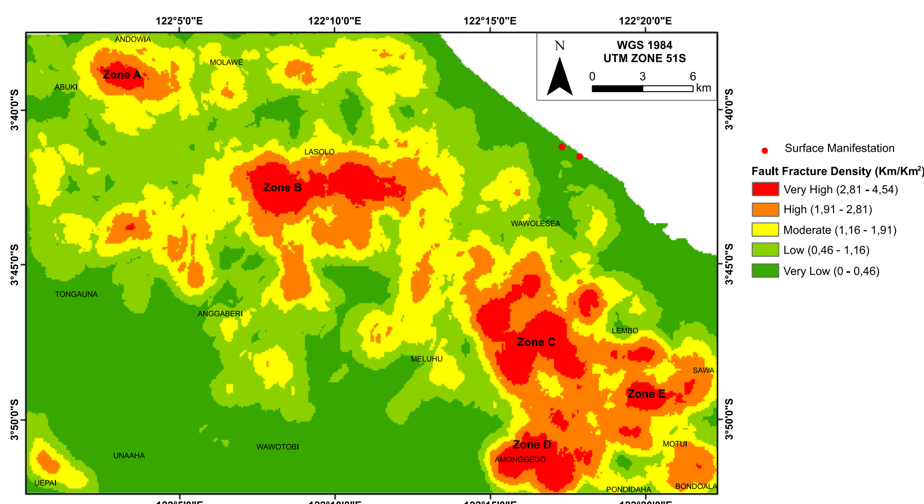

Fig. 10 Fault fracture density (FFD) in the study area

(zones), very high (2.81–4.54 km/km^2), high (1.91–2.81 km/km^2), moderate (1.61–1.91 km/km^2), low (0.46–1.61 km/km^2), and very low (0–0.46 km/km^2) (Fig. 10). Based on the planar area percentage, 5.74% of the research area shows a very high FFD value, followed by the other categories, 12.73%, 22.07%, 27.04%, and 32.02% for high, moderate, low, and very low FFD value category, respectively. The very high FFD is clustered in a total area of about 58.17 km^2. Complete results of descriptive FFD planar area measurement can be seen in Table 2.

The very high FFD values are spatially distributed along with the NW–SE pattern, surrounded by low-to-very low FFD areas with the same orientation (Fig. 10). Based on this, five zones were identified in the very high FFD area with a total area of about 2.85 km^2, 16.98 km^2, 19.39 km^2, 9.91 km^2, and 3.56 km^2, respectively, from zone A to zone E. The largest very high FFD value area is shown in zone C, located between Meluhu and Lembo, measured for about 19.39 km^2. Besides, zones C, D, and E are spatially connected by high FFD values. In contrast, although the southern part of Wawolesea is considered to have a high-to-very high FFD value, the northern part shows very low-to-moderate FFD values.

Field observations and measurements

Lithological intervals observed in the study area from on eight ground-truthing locations include schist as part of the Palaeozoic Metamorphic Formation, phyllite, marble and sandstone from the Meluhu Formation, and limestone of the Tokala Formation (Fig. 11).

Fractures were observed within the limestone interval of the Tokala Formation. Both open (unmineralized) and mineralized fractures were observed in the Meluhu sandstone Formation (Fig. 12). Mineralized fractures identified as two sets of silica veins trending NW–SE (set 1; Sv1) and NNE–SSW (set 2; Sv2). These silica-filled veins display an average aperture size of about 20.36 mm for set 1 and 14.23 mm for set 2 (Fig. 12a, b).

Based on outcrop-scale observation, the NW–SE set (set 1) that show high aperture sizes is crosscut by the thinner NNE–SSW set (set 2). Set 2 is also observed to be crosscut by N–S trending open fractures (Fig. 12a, b). In Meluhu Formation, phyllite and Marble were observed to have carbonate veins of NNE–SSW orientation (Fig. 12c–e). Phyllite foliation was crosscut by carbonate-filled veins. Full details of ground-truthing fracture measurements are shown in Table 1.

Discussion

Permeable zone in northern part of Konawe

Permeability of geothermal reservoirs is usually controlled by the density of fractures with various lengths and widths (Grant et al. 1982). High fault fracture density (FFD) values reflect the high number of faults and fractures in the study area (see Fig. 9 and Table 2) and indicate the presence of highly permeable zones within the area (Fig. 10). The lineaments distribution divides the study areas into five zones of very high FFD values (Fig. 13), implying zones of high permeability. Most of the permeable zones are spatially distributed in the Meluhu Formation, and only one permeable zone is present in the Tokala Formation. This result is consistent with the study of Rusmana et al. (1993), in which ten faults were observed in the Meluhu Formation, and only one fault is present

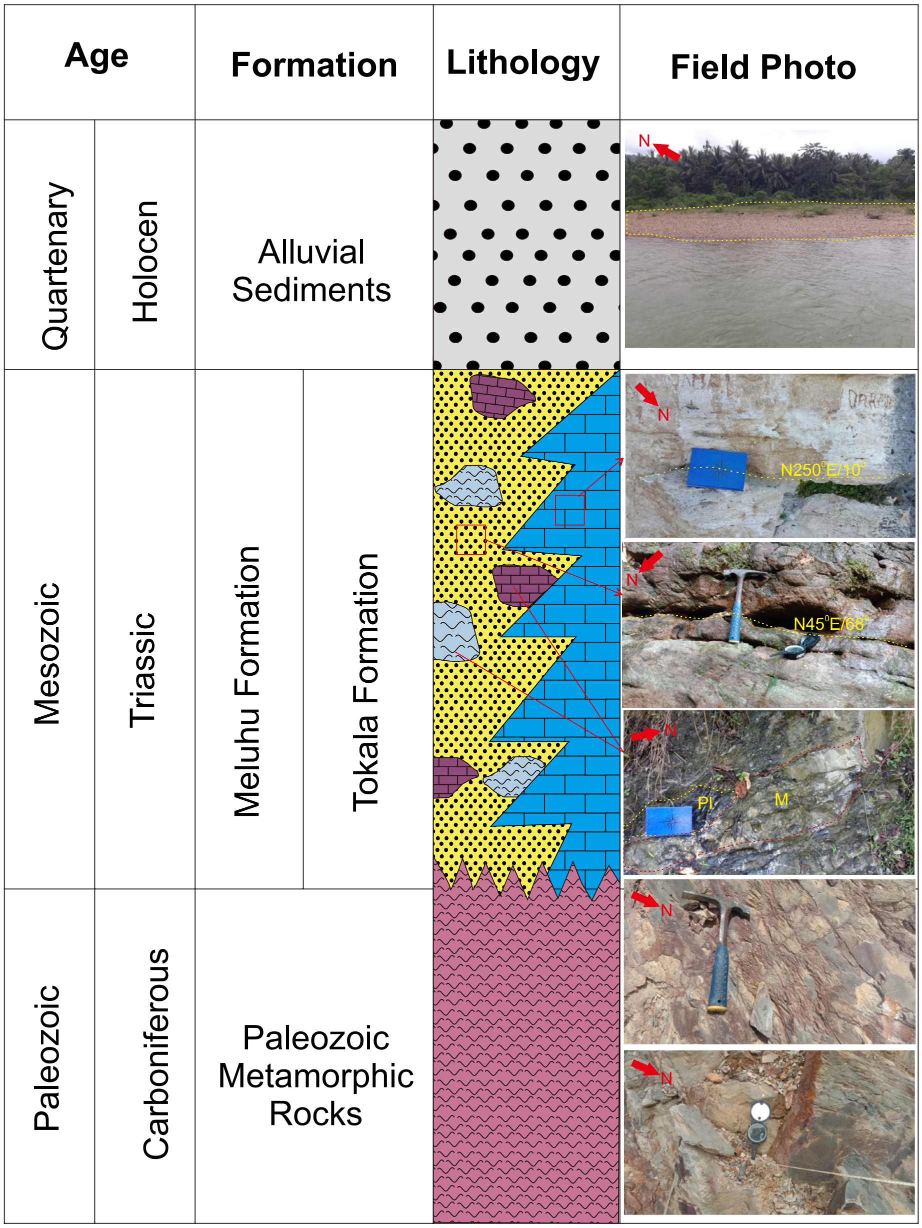

Fig. 11 Stratigraphic column of the study area

in the Tokala Formation. Based on ground-truthing, most of sandstone in the Meluhu Formation is relatively highly fractured compared to the limestone in the Tokala Formation and in the phyllite. This indicates the fluid will flow differently in each of these units. Figure 11 shows a columnar section of the study succession. The fractures (mainly open fractures) in the sandstone interval of the Meluhu Formation will act as a conduit to the thermal fluids, particularly if the fractures are interconnected and have good connectivity.

Fracture density measurements collected from the field are relatively consistent with the fracture density obtained through remote sensing. Ground truthing (GT) localities

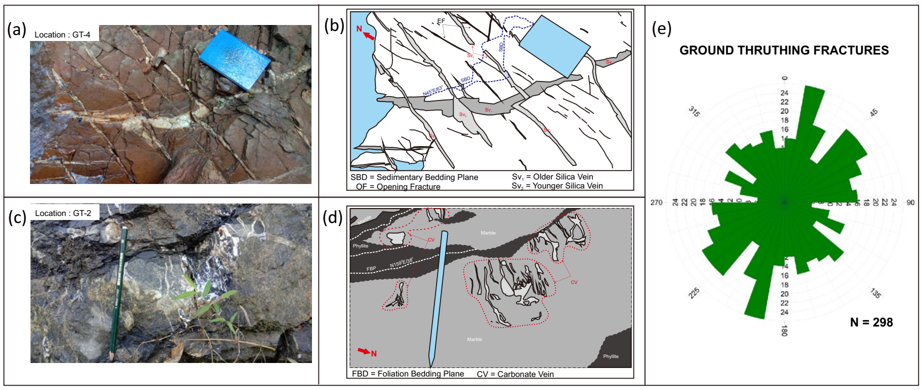

Fig. 12 Fracture observed and mapped in the study area. **a** Field photograph showing the different fracture sets observed in GT-4; **b** schematic drawing of **a**; **c** field photograph showing the fractures observed in of GT-2; **d** schematic drawing of **c**; **e** rose diagram showing the orientation of all fractures mapped in all ground-truthing locations

Table 2 Descriptive statistics FFD planar area measurements in five value categories in the study area

Category	FFD value	Largest area (km^2)	Least area (km^2)	Mean (km^2)	Total planar area (km^2)	Percentage (%)
Very high	2.81–4.54	19.39	0.01	1.76	58.17	5.74
High	1.91–2.81	66.45	0.01	2.26	129.01	12.73
Moderate	1.61–1.91	161.79	0.01	2.83	223.71	22.07
Low	0.46–1.61	260.00	0.01	6.47	278.17	27.44
Very low	0–0.46	236.97	0.01	5.15	324.63	32.02
Total planar area (km^2)					1013.69	100.00

GT-1 and GT-3 are not located within the high FFD zone (Fig. 13), indicating that no fractures were identified in these areas (Table 1). GT-7 is located where the Meluhu Formation is exposed, but it is not considered as a high FFD zone. Instead it shows relatively moderate fracture density (4.6 m^{-1}). GT-4 and GT-5 in the Meluhu Formation are considered high FFD zones. Based on field measurements, the density of the mapped fractures in these zones is relatively high compared to other locations, supporting the fracture data collected using remote sensing.

Since most of the faults and lineaments extracted using remote sensing and observed and mapped in the field are distributed within the sandstone of Meluhu Formation, secondary permeability in this formation is considered higher than that in the Tokala Formation, suggesting an improved fluid flow in the Meluhu formation. Besides, the largest permeable zone is located between Meluhu and Lembo (zone C in Fig. 13) with an area of 19.39 km^2. Moreover, based on the high FFD values, the southern part of Wawolesea (zones C, D, and E) is also considered as a permeable zone (Fig. 13).

Prospective geothermal reservoir

Non-volcanic geothermal systems could be assessed by the analysis of lineaments and fault and fracture density (Suryantini 2013; Nahli et al. 2016). This methods supported

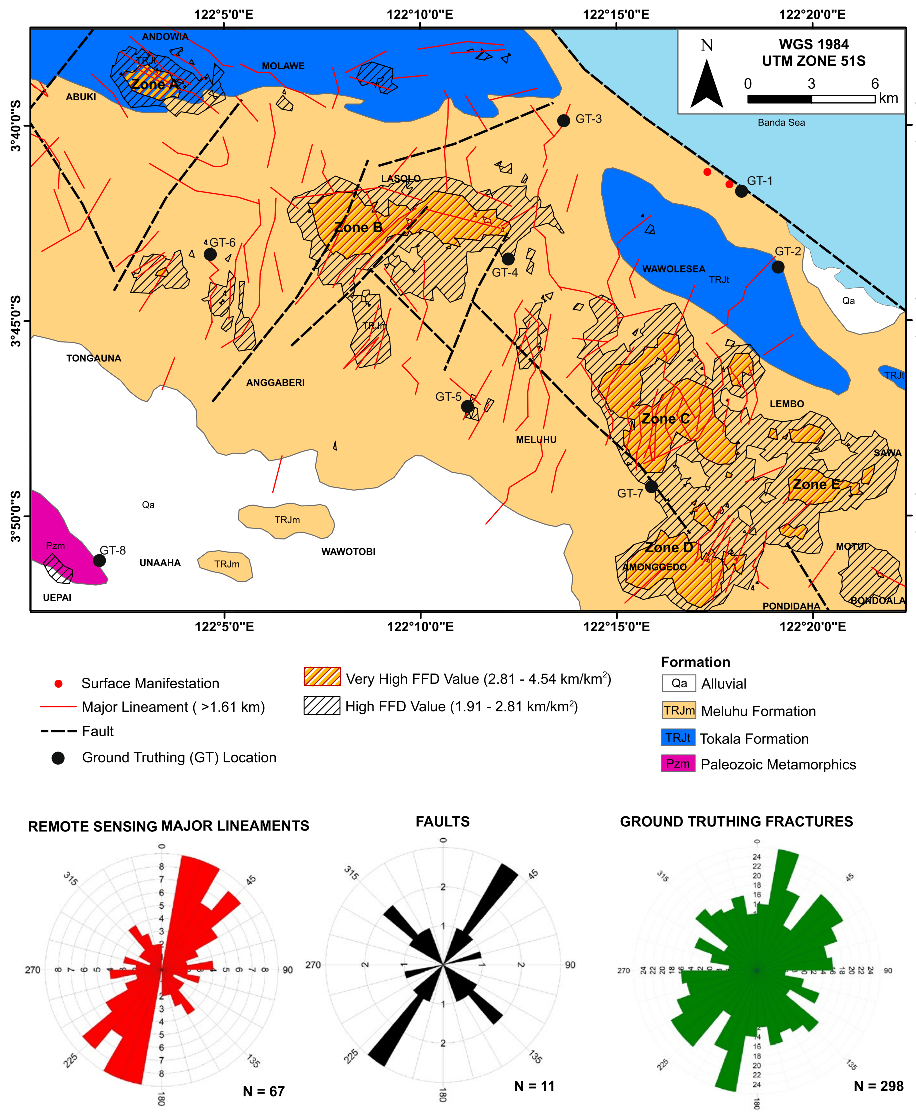

Fig. 13 Geological map of the study area with major lineaments and high–very high FFD values derived from lineament interpretation

by field measurements were applied to the non-volcanic geothermal system of Northern Konawe in order to identify the prospective geothermal reservoir.

Zone C, the zone located between Meluhu and Lembo, is the most prospective geothermal reservoir based on the total planar area, the orientation of major lineaments, and the field (ground-truthing) fracture measurements. The largest measured area for a very high FFD zone indicates larger area for fluid flow through fracture permeability. Therefore, zone C is considered the most prospective geothermal reservoir due to its large area (19.39 km^2) compared to other measured zones.

The rose diagram of major lineaments shows a NNE–SSW azimuth orientation, with a direction that corresponds to the quadrant of faults characterized by Rusmana et al. (1993) and the field fracture measurements collected from all study localities. If a line is drawn connecting surface manifestations and zone C, the line orientation would have the same quadrant of azimuth orientation with major lineaments and faults. Moreover, this is also in line with the results of the study by Jaya et al. (2021), where the land surface temperature (LST) map shows a high anomalous temperature from the northeast part of Wawolesea to the southwest direction (Fig. 4). Therefore, it is believed that the geothermal fluid flows from the area between Meluhu and Lembo to the surface manifestations in the northeast part of Wawolesea.

Although the study by Rusmana et al. (1993) shows intense faults around zone B which indicates a permeable zone within the area, the orientation and connection of fractures correspond less to surface manifestations. Four faults in zone B have NE–SW and NW–SE trends. If drawn from Zone B, the orientations show no termination towards the surface manifestation. Moreover, the observed connection of faults shows that the flow of fluid is from zone B to zone C, suggesting that zone B supplies fluid to zone C, the area between Meluhu and Lembo.

Based on field fracture measurements, most of the fractures trending NNE–SSW within the study area are mineralized, indicating mineral deposition from hydrothermal fluids (Edwards and Atkinson 1985) in the fractures that are relatively not able to conduct fluid flow anymore. However, new opening-mode fractures developed as shown by the two sets of silica veins that are crosscut N–S by open fracture at GT-4 (Fig. 6b). Moreover, GT-7 shows the same orientation of open fractures. The N–S trending opening fractures within the study area (Fig. 13) align with the southeastern Sulawesi N and NW collision vector direction that evolved during Miocene through Pliocene (Sompton 2012). The collision is interpreted to be controlling the the formation of N–S open fractures in the Triassic Sandstone of the Meluhu Formation. Despite the slight difference in orientation between the major lineaments and faults extracted using remote sensing and the fractures measured/mapped in the field, most the fractures terminate at the Wawolesea surface manifestations.

Conclusions

This study has investigated high permeable zones in the non-volcanic geothermal system of Northern Konawe using lineament and fault fracture density (FFD). The conclusions of this study can be summarized as follows:

- A total of 1694 lineaments (major and minor) were extracted in the research area from DEMNAS data.
- Major lineaments (more than 1.61 km in length) show a NNE–SSW trend, while minor lineaments (less than 1.61 km in length) show a non-aligned arrangement. The fluid source of surface manifestations comes from its SSW direction (the orientation of major lineaments azimuth).
- Five zones are considered to be permeable in the research area.
- The area between Meluhu and Lembo is believed to be the most prospective geothermal reservoir due to having the largest planar permeable area and an exact location for the SSW direction of surface manifestations.

Further detailed exploration including geological modeling of subsurface fractures and faults along prospective reservoir geothermal area is highly recommended.

Abbreviations

DEMNAS Digital Elevation Model Nasional
FFD Fault fracture density
LST Land surface temperature

Acknowledgements

The authors thank the College of Petroleum Engineering and Geosciences (CPG), King Fahd University of Petroleum and Minerals (KFUPM) for providing the financial support to conduct this research. We thank the reviewers for the insightful comments and the positive assessment of our paper.

Author contributions

DA: conceptualization, data curation, formal analysis, investigation, methodology, validation, visualization, writing. ISA: conceptualization, investigation, methodology, supervision, validation, visualization, writing—review and editing. SDP: data curation, investigation, methodology, validation, visualization. All authors read and approved the final manuscript.

Funding

This research is funded by King Fahd University of Petroleum and Minerals (KFUPM), Saudi Arabia.

Availability of data and materials

Data supporting the findings are available from the authors upon request.

Declarations

Competing interests

There are no competing interests.

Received: 9 June 2022 Accepted: 28 November 2022
Published online: 17 December 2022

References

Abdelkareem M, Al-Arifi N. Synergy of remote sensing data for exploring hydrothermal mineral resources using gis-based fuzzy logic approach. Remote Sens. 2021;13:4492. https://doi.org/10.3390/rs13224492.
Allum JAE. Lineament, linear, lineation: some proposed new standards for old terms: discussion. Bull Geol Soc Am. 1978;89:159–159. https://doi.org/10.1130/0016-7606(1978)89%3c159a:LLLSPN%3e2.0.CO;2.
Aulia RN, Nur I, Ilyas A. ANALISIS GEOKIMIA AIR PANAS DAERAH WAWOLESEA. Jurnal Geocelebes. 2022;6: 64–71. https://doi.org/10.20956/geocelebes.v6i1.19672.
BIG. Seamless digital elevation model (DEM) dan Batimetri Nasional [WWW document]. Badan Inf. Geospasial. 2018. https://tanahair.indonesia.go.id/demnas/. Accessed 23 Jan 2022.
Chen BC, Perdana T, Kuo LW. Fluid flow and fault-related subsurface fractures in slate and metasandstone formations: a case study of the Jentse Geothermal Area, Taiwan. Geothermics. 2021;89: 101986. https://doi.org/10.1016/j.geothermics.2020.101986.
Dasgupta S, Mukherjee S. Remote sensing in lineament identification: examples from western India. In: Problems and solutions in structural geology and tectonics. 1st ed. Amsterdam: Elsevier Inc.; 2019. https://doi.org/10.1016/b978-0-12-814048-2.00016-8.
Dickson MH, Fanelli M. What is geothermal energy? International Geothermal Association (IGA); 2004. p. 1–33. http://iga.igg.cnr.it/geo/geoenergy.php.
Edwards R. Atkinson, K. Ore Deposit Geology And Its Influence on Mineral Exploration. 1985. London: London New York Chapman and Hall.
Fisher GB, Amos CB, Bookhagen B, Burbank DW, Godard V. Channel widths, landslides, faults, and beyond: the new world order of high-spatial resolution Google Earth imagery in the study of earth surface processes. Geol Soc Am Spec Pap. 2012;492:1–22. https://doi.org/10.1130/2012.2492(01).
Grant MA, Donaldson IG, Bixley PF. Geothermal reservoir engineering. New York: Academic Press; 1982. p. 369.
Hamimu L, Ngkoimani LO, Jahidin J, Asfar S, Usmardin U. Analysis of the sub-surface distribution of graphite minerals using the geoelectrical resistivity method in the Sabilambo Village, Kolaka Regency, Southeast Sulawesi Province. J Geosci Eng Environ Technol. 2019;4:149. https://doi.org/10.25299/jgeet.2019.4.3.2406.
Idral A. Potency of non volcanic hosted geothermal resources in Sulawesi-Indonesia. In: World Geothermal Congress; 2010. p. 25–9.
Jamaluddin, Umar EP. karakteristik fisik dan kimia mataair panas daerah barasanga kabupaten konawe utara. Jurnal Geocelebes. 2017; 1, pp. 62–65. https://doi.org/10.20956/geocelebes.v1i2.2291.
Jaya LMG, Suprayogi A, Sudarsono, Hasbi M. Identification of non-volcanic geothermal manifestation in North Konawe Regency Indonesia using land surface temperature of Landsat satellite image. IOP Conf Ser Earth Environ Sci. 2021;622: 012040. https://doi.org/10.1088/1755-1315/622/1/012040.
Laubach SE, Lamarche J, Gauthier BDM, Dunne WM, Sanderson DJ. Spatial arrangement of faults and opening-mode fractures. J Struct Geol. 2018;108:2–15. https://doi.org/10.1016/j.jsg.2017.08.008.
Manzella A. Geothermal energy. EPJ Web Conf. 2017;148:1–26. https://doi.org/10.1051/epjconf/201714800012.
Martosuwito S. Tectonostratigraphy of the eastern part of Sulawesi, Indonesia. In relation to the terrane origins. J Geol Dan Sumberd Miner. 2012;22:199–207.

Microsoft Bing. Satellite image of the northern part of Konawe [WWW document]. 2022. https://www.bing.com/maps/aerial. Accessed 19 Feb 2022.
Nahli K, Mulyana F, Tsani GE, Alwan MA, Darojat MH, Hendrawan RN. Identifying non-volcanic geothermal potential in Amohola, Southeast Sulawesi Province, by applying the fault and fracture density (FFD) Method. IOP Conf Ser Earth Environ Sci. 2016. https://doi.org/10.1088/1755-1315/42/1/012015.
Naivasha L. Geothermal systems in a global perspective. 2015. p. 1–12.
Osaragi T. Classification methods for spatial data representation. Center for Advanced Spatial Analysis, vol. 44. London: University College London; 2002. p. 1–19.
Prost GL. Remote sensing for geoscientists. Remote Sens Geosci. 2013. https://doi.org/10.1201/b15638.
Rusmana E, Sukarna D, Haryono E, Simandjuntak TO, et al. Geological map of Lasusua Kendari Quadrangles, Sulawesi-Scale 1: 250.000. Transverse Mercator Projection, Copy Right: Pusat Penelitian dan Pengembangan Geologi; 1993.
Sarp G. Lineament analysis from satellite images, North-West of Ankara. Ankara: Middle East Technical University; 2005.
Sompton AF. Struktur Geoligi Sulawesi. Bandung: Perpustakaan Sains Kebumian Institut Teknologi Bandung. 2012
Siler DL, Faulds JE, Hinz NH, Dering GM, Edwards JH, Mayhew B. Three-dimensional geologic mapping to assess geothermal potential: examples from Nevada and Oregon. Geotherm Energy. 2019;7:1–32. https://doi.org/10.1186/s40517-018-0117-0.
Simandjuntak TO, Surono S. Peta Geologi Lembar Kolaka, Sulawesi. Pusat Penelitian dan Pengembangan Geologi. 1993.
Suharmanto P, Fitria AN, Ghaliyah S. Indonesian geothermal energy potential as source of alternative energy power plant. KnE Energy. 2015;1:119. https://doi.org/10.18502/ken.v1i1.325.
Surono TO, Simandjuntak RL. Peta Geologi Lembar Batui, Sulawesi. 1993.
Suryantini. Statistical analysis of mercury data from soil survey in non-volcanic geothermal system: a case study in Sulawesi. Procedia Earth Planet Sci. 2013;6:212–8. https://doi.org/10.1016/j.proeps.2013.01.029.
Suryantini, Wibowo H. Application of fault and fracture density (FFD) method for geothermal exploration in non-volcanic geothermal system; a case study in Sulawesi-Indonesia. In: Proceeding world geothermal congress. 2010. p. 25–9.
Tjokrosapoetra S, Budhitresna T, Rusmana E. Peta Geologi Lembar Buru, Maluku. 1993.
USGS. USGS EROS archive—digital elevation—shuttle radar topography mission (SRTM) 1 arc-second global [WWW document]. Earth Resources Observation and Science (EROS) Center. 2018. https://www.usgs.gov/centers/eros/science/usgs-eros-archive-digital-elevation-shuttle-radar-topography-mission-srtm-1-arc?qt-science_center_objects=0#qt-science_center_objects. Accessed 24 Jan 2022.

Publisher's Note

Springer Nature remains neutral with regard to jurisdictional claims in published maps and institutional affiliations.